Energy loss of protons and helium ions passing through matter

Toshiaki Kaneko
Department of Applied Physics, Okayama University of Science, Ridai-cho 1-1, Okayama 700, Japan
(Received 19 July 1985)

Based on the dielectric-function method, together with the use of local-electron-density models (LEDM's), the stopping powers of solid materials for the proton and helium-ion beams are investigated over a wide specific energy range from 1 keV/amu to 2.5×10^3 keV/amu. The screening effect due to free electrons on ions with bound electrons is taken into account within the framework of the linear response. For a H^0 atom in alkali metals, the screening effect increases significantly the stopping powers, while for a He^+ ion it does not increase so much. The mean excitation energy is also calculated using the solid and the atomic LEDM's. For a Ag target, not being a simple metal, we report how much the change in the number of free electrons affects the stopping cross section for a H^+ ion. The charge-state distribution (CSD) suggested from the master curves of compiled stopping data is in agreement with the observed CSD. The calculated energy dependence of the effective charge of the helium-ion beams reproduces experimental data well.

I. INTRODUCTION

The slowing down and the charge-state population of energetic ions traversing matter have been one of the main problems in atomic collision phenomena in solids for many years. Accurate estimation of the energy loss of protons and helium ions plays an essential role in analyzing the depth profile of impurity atoms in ion implantation. So far, the data compilations have been performed comprehensively so that we can get some general features in the processes of slowing down[1] and charge distribution.[2] Some authors have given their theories of the electronic stopping powers of matter for point-charge intruders, based on either atomic collision methods[3–5] or the dielectric-function method.[6] The dielectric-function method has been extended for a partially stripped ion.[7] Besides the target-excitation process, the contribution of the projectile-excitation process to the stopping cross sections has been discussed within the first Born approximation.[8] For heavy ions with intermediate velocities, the effective-charge model discussed intensively by Brandt and co-workers[9] is particularly useful to summarize successfully a large amount of stopping-cross-section data. Judging from those data, the effective charge does not depend strongly upon target materials with atomic number Z_2. In the case of helium ions, the weak Z_2 dependence of the effective charge does not directly imply that of the average charge inside matter. Actually, as for MeV helium-ion beams, this weak target dependence was reconciled with the strong Z_2 oscillations in the average charge by taking into account the equilibrium charge-state population in matter and the spatial size of a He^+ ion.[10]

From practical points of view, the local-electron-density model (LEDM) for describing the spatial distribution of the target electrons and the related physical quantities is often used successfully to estimate the stopping cross sections for a single particle. For atomic targets, the LEDM is easily obtained, for example, by using Hartree-Fock wave functions,[11] while for solid targets it should be modified in such a way that free electrons are included. To satisfy this request as simply as possible, we assume the electron density constant in the outer region of the Wigner-Seitz (WS) cell. This constant density is characterized by the bulk plasma frequency.[12] Although it is a crucial approximation, this method is similar to band-structure calculation by means of the Korringa-Kohn-Rostoker (KKR) method in that the potential is divided into two regions in order to separate corelike and freelike wave functions in the WS cell.

The charge-state distribution of a proton beam and a helium-ion beam in solids has been discussed for several decades.[13] To count the number of allowed charge states, we are faced with the historical problem of how many bound states can exist stably in the ion inside solids. Following Rogers *et al.*,[14] the number of stable bound states n^* in the screened Coulomb potential is found approximately to be

$$n^*=0.5829+0.4993DZ_1/a_0\ , \tag{1.1}$$

where Z_1 and D denote the nuclear charge of the ion and the screening length of the potential, respectively. Recently, by using the many-body technique, Guinea *et al.*[15] have formulated the equilibrium charge of a proton and a helium ion traversing an electron gas, in terms of the correlation self-energy corresponding to the electron transition from (to) the conduction band to (from) the hole created in the ion. This procedure is considered as an extension of the idea of Cross,[16] who shows the equilibrium charge state of a proton in a solid is determined by the electron-capture and -loss cross sections obtained for the same target element in a gaseous phase. His opinion is valid at higher velocities than the Fermi velocity v_F, since the core electrons play a more dominant role than free electrons in the processes of electron capture and loss. At lower velocities than v_F, however, free electrons become important in determining the equilibrium charge in terms of the energy-level broadening of the bound states in the ion, which is caused by the resonance electron capture and

the collisional electron loss.[17]

The aim of this paper is to evaluate the stopping cross sections of solid media for proton and helium-ion beams as an extension of previous work.[10] The stopping cross sections for a single particle, whether it is a point charge or not, are calculated on the basis of the Lindhard-Winther theory together with the LEDM. The effective charges are also calculated using the charge-state fractions suggested from the stopping data. We show the difference in the mean excitation energy by using the atomic LEDM and the solid one. The screening effect is taken into account within the linear response. In Sec. II the basis of calculation is described briefly, and Sec. III presents the results and discussions. The conclusion is given in Sec. IV. Throughout the paper, atomic units are used unless stated otherwise.

II. BASIS OF CALCULATION

When an ion beam passes through solids and gaseous targets, it is allowed to have several charge states inside them. Provided that the charge-state distribution (CSD) is not rearranged after emerging, the observed CSD directly reflects the CSD inside matter. In the case of heavy ions emerging from foils, the post-foil CSD is not necessarily the same as the CSD inside foils. This effect is explained by the Auger deexcitation process after emerging. As we concentrate on the energy loss of ions inside matter, the post-foil CSD is not considered in the formulation of this paper. Including the charge states in the transport problem,[18] our starting formula for the stopping of matter for ion beams is given as follows:

$$S=\sum_i \phi(i;x)S_i,\quad S_i=\int_0^\infty d\omega\,\omega P_i(\omega)\,, \tag{2.1}$$

where $P_i(\omega)d\omega$ is the excitation probability per unit length between excitation energies ω and $\omega+d\omega$. Equation (2.1) means that the stopping power of matter for ion beams is obtained by averaging that for a single particle over allowed charge-state fractions in matter. In general, as the particles traverse, their charge-state distribution is equilibrated. Then the charge fraction at depth x, $\phi(i;x)$, in (2.1) reduces to its equilibrated value $\phi(i;\infty)$. The path length L, at which the CSD attains equilibrium, depends upon the magnitude of the charge-changing cross sections, σ_{ij}'s, from charge state j to i. In the case of H or He with two dominant charge states, e.g., labeled 0 and 1, at any velocities, L is nearly equal to $(\sigma_{01}+\sigma_{10})^{-1}N^{-1}$, where N is the number density of target atoms. Except for surface scattering techniques measuring the outgoing particles colliding with the surface atoms, most measurements of energy loss are performed under the charge equilibrium condition. Moreover, in view of the comparison of the theoretical results with the experimental ones, we may neglect a thin "nonequilibrium" region with its depth L in comparison with a thick "equilibrium" region of target materials.

As for the stopping power for a particle in a particular charge state i, S_i, with atomic number Z_1 and velocity v, is given by the dielectric-function theory, extended for a partially stripped ion. The stopping power of a free-electron gas is then found to be

$$S_i=n\int_0^\infty d\omega\,\omega\int_{\omega/v}^\infty dk\,(2/k\pi v^2)\,|\,Z_1-\rho_i(k)\,|^2 \times \mathrm{Im}[\,1/\epsilon(k,\omega)\,]\,, \tag{2.2}$$

where n and $\epsilon(k,\omega)$ denote the number density of free electrons and the dielectric function of the media, respectively. The spatial distribution of the bound electrons, $\rho_i(r)$, in the ion is assumed to be spherically symmetric so that its Fourier transform $\rho_i(k)$ has the same symmetry. As regards H and He, $\rho_i(r)$ is calculated from the hydrogenic $1s$ orbital. As is well known, the imaginary part of $\epsilon^{-1}(k,\omega)$ is contributed both from the electron-hole pair excitation branch and from the collective excitation branch. These contributions are both evaluated numerically.

The LEDM's are used from practical points of view to calculate the stopping power S_i and the mean excitation energy I. For atomic targets, the spatial electron densities are described by Hartree-Fock (HF) wave functions. Thus we easily use the atomic LEDM. On the other hand, in the solid LEDM, the electron density in the outer region of the WS cell is assumed to be constant, for simplicity, for describing the free electrons. Their collective motion is characterized by the bulk plasma frequency ω_p.[12] In this case a correction term is needed to conserve the total number of electrons in the WS cell, since the electron density in the inner region of the WS cell is still described by HF wave functions.

The induced polarization of a free-electron gas screens the electric field provided by a moving charged particle. In the Thomas-Fermi model of a degenerated electron gas, the screened potential is spherically symmetric and of the form

$$V(r)=-Z_1\exp(-k_c r)/r,\quad k_c=(12/\pi)^{1/3}r_s^{-1/2}\,, \tag{2.3}$$

in atomic units, for the case $v\ll v_F$. In the above, r_s is the radius of a sphere occupied by one electron measured in units of the Bohr radius a_0. This screening effect resultantly weakens the binding force applied to the bound electron in a H^0 or a He^+ so that the orbital radius is enlarged more than in the case of no screening. The extended orbital radius a_1 is determined by minimizing the expectation value of the binding energy $\langle E_b\rangle$ with respect to a_1: $\partial\langle E_b\rangle/\partial a_1=0$. Within the first-order perturbation, $\langle E_b\rangle$ is given as

$$\langle E_b\rangle=(2a_1^2)^{-1}-(Z_1/a_1)(1+a_1k_c/2)^{-2}\,. \tag{2.4}$$

We assume here the hydrogenic $1s$ wave function of the form $\psi(r)=(\pi a_1^3)^{-1/2}\exp(-r/a_1)$ $(a_1=1/Z_1)$ to describe the bound electron in a H^0 or a He^+. Unless the screening is taken into account, i.e., $k_c=0$, then $a_1=1.0$ for a H^0 and 0.5 for a He^+, in atomic units. Due to the extension of a_1, the external charge in the Fourier space, i.e., $Z_1-\rho_i(k)$, results in being effectively greater than that in the vacuum.

One of the basic points is to include the charge-state distribution of ion beams inside matter in calculation of the stopping powers. In a free-electron gas the screening length D is given as $D=k_c^{-1}$ within the linear screening, so that Eq. (1.1) allows us to get the number of stable bound states in the particle. When we set $n^*=1$ with

$Z_1=1$ and $n^*=2$ with $Z_1=2$, we obtain $r_s=1.70$ and 4.92, respectively. This means that a proton inside solids with $r_s<1.70$ cannot bind any electrons stably and also means that two electrons cannot be bound in a helium ion inside solids with $r_s<4.92$. Therefore, it is enough to consider the fractions of protons and singly and doubly ionized helium ions inside solids except for alkali and alkaline-earth metals.[19]

Equation (2.1) implies that if we can calculate reasonably the stopping cross sections for ions in each charge state, we infer the CSD from the master curves of the data obtained experimentally on the stopping cross sections for the ion beams. Fortunately, as regards H and He, many data have been reported and such available data covers a wide energy range of interest per nucleon from 1 keV/amu to 2.5×10^3 keV/amu. The charge fraction data for light ions are well arranged as a function of the energy E in the form

$$\phi_i/\phi_j=AE^{-B}, \tag{2.5}$$

where A and B are parameters. This energy dependence of the charge fraction ratio is actually valid except at low specific energies less than ~10 keV/amu. We show later the comparison between the predicted CSD from the master stopping curves and the measured CSD.

III. NUMERICAL RESULTS AND DISCUSSIONS

First, as an example, we show in Fig. 1 the calculated stopping cross section of Al for a H^+ and a He^+, denoted by S_{H^+} and S_{He^+}, respectively, in the solid LEDM. Except for the maximum stopping region, the calculated S_{H^+} agrees with the data.[20–30] We assume that there are three free electrons per Al atom participating in the conduction band. This is consistent with the number of conduction electrons deduced from the observed ω_p. As well as S_{H^+}, S_{He^+} can be easily calculated over the whole energy range within the linear response on the basis of the LEDM. Compared with S_{H^+}, the specific energy at the peak of S_{He^+} is a bit shifted toward a large keV/amu region. Moreover, the S_{He^+} curve has a broader hump than the S_{H^+} curve. We note that the screening effect on a He^+ is not included here.

In Fig. 2 the ratios of the stopping cross sections, i.e., S_{He^+}/S_{H^+} versus specific energy E (keV/amu) are illustrated for various targets. At a glance, we can see the remarkable feature. That is, in the lower-energy region $E\lesssim60$ keV/amu, the ratio is nearly constant. Beyond ~60 keV/amu, it increases rapidly and at last saturates in the high-energy region. This behavior is explained by the following. At low velocities ($v<v_F$), a momentum-transfer region $0<k<2k_F$ contributes dominantly to the integral in (2.2) almost regardless of v. According to rigorous calculations of the stopping of a uniform electron gas,[6,7] S_{H^+} and S_{He^+} are proportional to v at low velocities. Besides the magnitude of a factor, this velocity dependence is still preserved even if we adopt the LEDM. With increasing velocity ($v>v_F$), free electrons are scattered rather by the nucleus of the ion and resultantly the contribution of a large momentum-transfer region, depending on v, becomes significant. In this region, $Z_1-\rho_i(k)$ approaches 2, and consequently a He^+ tends to behave like a He^{2+}. Thus the orbital size effect on S_{He^+} is vanishing as the velocity increases. Such a velocity dependence of S_{He^+}/S_{H^+} is expected for all solid targets

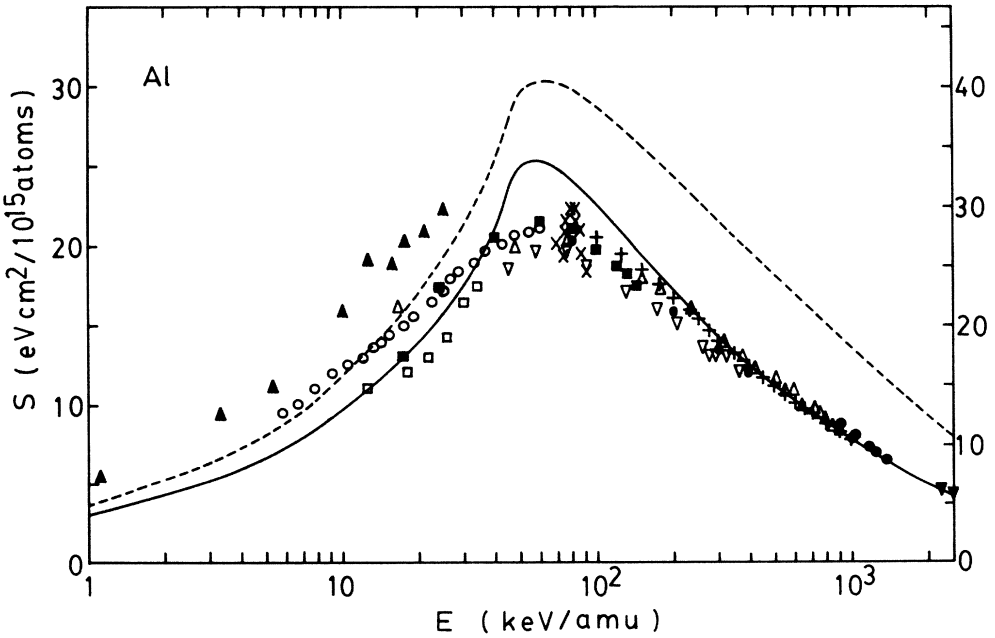

FIG. 1. Stopping cross sections of Al: the experimental results for a H^+ (×, Ref. 20; ○, Ref. 21; ▽, Ref. 22; △, Ref. 23; ▼, Ref. 24; □, Ref. 25; ■, Ref. 26; ●, Ref. 27; ▲, Ref. 28; +, Ref. 29; ⬮, Ref. 30) and the theoretical results [—— for a H^+ (left vertical axis) and — — — for a He^+ (right vertical axis)].

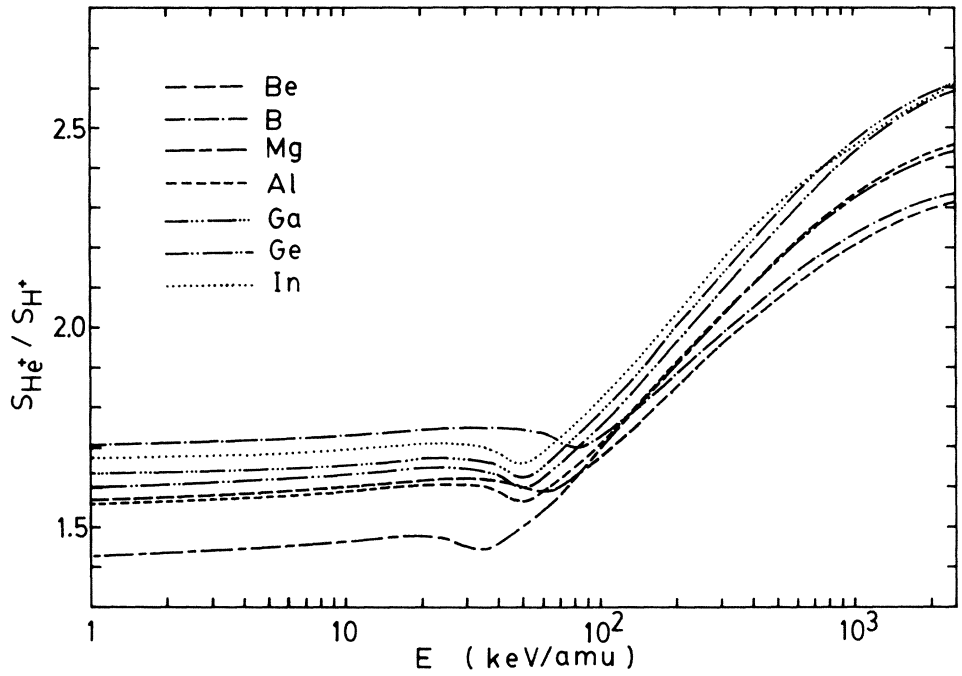

FIG. 2. Ratios of the stopping cross sections, S_{He^+}/S_{H^+}, vs specific energy for various solids.

considered here so that it can be regarded as a general feature. As will be seen later, this trend plays a decisive role in the effective charge q_{eff} for low-energy helium-ion beams. Small hollows around the specific energies corresponding to the maximum stoppings are caused by the appearance of the collective excitation branch.

The screening effect increases the stopping cross section S_{He^+} through the enlargement of orbital radius a_1. We denote by $S^*_{He^+}$ the stopping cross section for a He^+ ion in the case of including the screening effect. The calculated ratio $S^*_{He^+}/S_{He^+}$, tabulated in Table I, is almost independent of the velocity v in the $v \lesssim v_0$ (v_0 is the Bohr velocity) region. There, the stopping cross sections increase by about 10% for a He^+.

To examine the Z_2 dependence of S_{H^+} at a low velocity, the calculated result is shown in Fig. 3, where we assume the number of free electrons per atom to be one for $_3$Li, $_{11}$Na, $_{19}$K, $_{29}$Cu, $_{37}$Rb and $_{47}$Ag; two for $_4$Be, $_{12}$Mg, $_{20}$Ca, $_{22}$Ti, $_{23}$V, $_{25}$Mn, $_{26}$Fe, $_{27}$Co, $_{28}$Ni, $_{30}$Zn, $_{38}$Sr, $_{46}$Pd, and $_{48}$Cd; three for $_5$B, $_{13}$Al, $_{21}$Sc, $_{24}$Cr, $_{31}$Ga, $_{33}$As, $_{39}$Y, $_{41}$Nb, $_{45}$Rh, and $_{49}$In; four for $_6$C, $_{14}$Si, $_{32}$Ge, $_{34}$Se, $_{40}$Zr, $_{44}$Ru, $_{50}$Sn, and $_{52}$Te; and five for $_{51}$Sb. As regards alkali and alkaline-earth metals, the stopping cross sections for a hydrogen atom are also calculated in consideration of the screening effect, in which calculated orbital radii a_1's of the bound state in a H^0 in such metals are tabulated in Table II. Apart from the magnitude of the cross sections, the phase of oscillation is in good agreement with the values[1] suggested empirically. In the high-energy region $E \gtrsim 200$ keV/amu, the well-known Z_2 oscillations in S_{H^+} have been reported by several authors and, in addition, the difference in S_{H^+} calculated both by the atomic LEDM and by the solid one is very small for solid targets. However, at low energies the atomic LEDM yields both unreasonably large stopping cross sections and incorrect energy dependences.[12] These discrepancies come from the

TABLE I. Orbital radius a_1 in the screened Coulomb potential (2.3) of $Z_1=2$ (He), and the calculated stopping ratio $S^*_{He^+}/S_{He^+}$ for solids (also see text).

Element	$_4$Be	$_5$B	$_{12}$Mg	$_{13}$Al	$_{31}$Ga	$_{32}$Ge	$_{49}$In
N_f[a]	2	3	2	3	3	4	3
r_s[b]	1.822	1.537	2.515	1.985	2.009	1.973	2.056
a_1 (a_0)	0.599	0.619	0.570	0.590	0.589	0.590	0.587
$S^*_{He^+}/S_{He^+}$[c]	1.12	1.15	1.07	1.10	1.10	1.10	1.10

[a]The number of free electrons per atom.

[b]In this case, r_s values are a bit smaller than those obtained from a free-electron gas model, since the spatial region allowed for free electrons is a bit smaller by the inner volume of the WS cell if the same ω_p values are used.

[c]$S^*_{He^+}$ and S_{He^+} are the stoppings for a He^+, inclusive of and exclusive of the screening effect, respectively. These ratios are constant without respect to v in $v \lesssim v_0$.

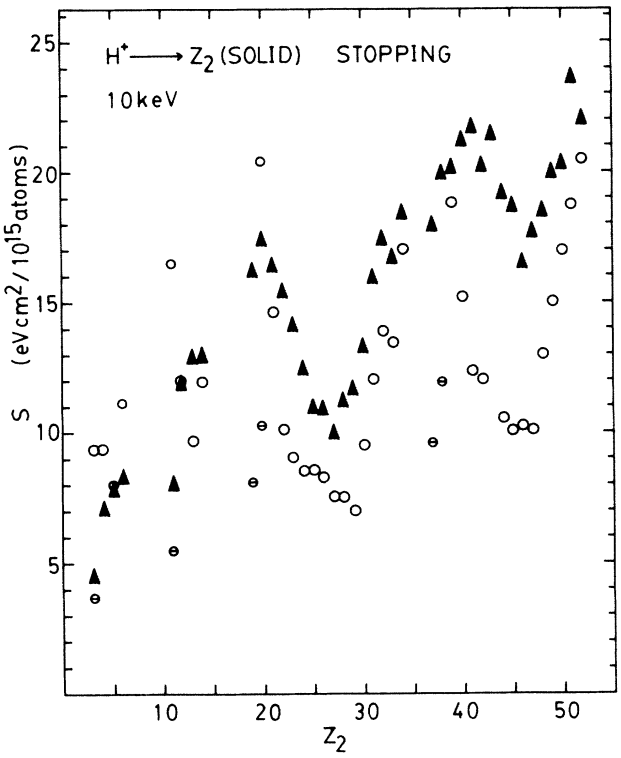

FIG. 3. Calculated stopping cross sections for a H^+ (○) and for a H^0 (Θ) vs Z_2 number at 10 keV together with the empirical values (Ref. 1) for a H^+ (▲).

TABLE II. Orbital radius a_1 in the screened Coulomb potential (2.3) of $Z_1=1$ (H).

Element	$_3$Li	$_{11}$Na	$_{19}$K	$_{20}$Ca	$_{37}$Rb	$_{38}$Sr
N_f[a]	1	1	1	2	1	2
r_s[a]	3.151	3.736	4.443	2.958	4.517	3.162
a_1 (a_0)	1.579	1.444	1.351	1.647	1.334	1.575

[a]See comments a and b in Table I.

tail part of the local electron density of a neutral atom. The electron density is so dilute there that the statistical model breaks down. Moreover, the ion velocity is, however small it is, regarded as "high" compared with the local Fermi velocity $v_F(r)$ ($=[3\pi^2\rho(r)]^{1/3}$) in the tail. In other words, this is caused by the fact that there is no excitation threshold appearing in the atomic LEDM, as was pointed out.[31] On the other hand, the solid LEDM actually has the excitation threshold corresponding to the resonance frequency ω_p. This difference is significant in obtaining reasonable stopping cross sections, especially at low energies. An important question regarding the solid LEDM is how to define the excitation threshold reasonably for solids. As concerns simple metals, this task is easy because the observed ω_p corresponds well to the theoretically predicted ω_p. For nonsimple metals, however, the situation is converse. As an example, the stopping cross section of a noble metal Ag for a proton is shown in Fig. 4, where the effective number of free electrons per atom,

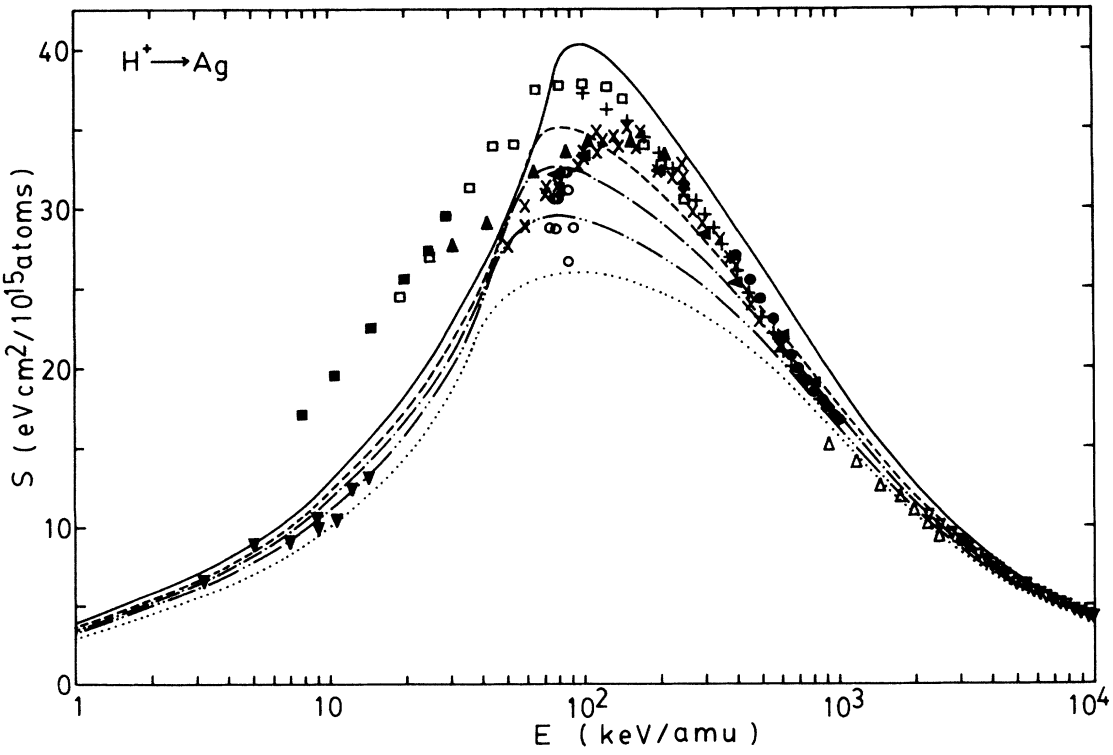

FIG. 4. Stopping cross sections of Ag for a H^+: the present results (—— for $\omega_p=25.0$ eV, – – – for 20.76 eV, —·— for 18.83 eV, —··— for 16.75 eV, and · · · · for 14.58 eV) and the experimental results (○, Ref. 20; ▽, Ref. 24; ■, Ref. 25; +, Ref. 29; ◀, Ref. 30; □, Ref. 32; ●, Ref. 33; ▲, Ref. 34; △, Ref. 35; ▼, Ref. 36; ×, Ref. 37).

N_{eff}, is treated as a parameter. The calculation was performed for five cases such that $N_{\text{eff}}=1$ ($\omega_p=14.58$ eV), 2 (16.75 eV), 3 (18.83 eV), 4 (20.76 eV), and 6.56 (25.0 eV). The figure shows that the variation of N_{eff} yields a dramatic change in S_{H^+} around the stopping maximum located at about 100 keV/amu. In contrast to such energies, there are not differences as large appearing in the higher- and the lower-energy regions. To explain this situation qualitatively, it is convenient to consider the local Fermi velocity $v_F(r)$, schematic forms of which are drawn in Fig. 5. At a high velocity v_h, the local Fermi velocity $v_F(r)$ is smaller than v_h in almost all WS space. Therefore, even if we change the excitation threshold a bit, no sensitive variation can be brought in S_{H^+}. Conversely, at a low velocity v_l, $v_F(v)$ is always larger than v_l without regard to N_{eff} more than 1. Then the result is also insensitive to N_{eff}. At an intermediate velocity v_m, however, the variation of N_{eff} affects greatly the size of the spatial region where the condition $v_F(r)>v_m$ [or $v_F(r)<v_m$] is satisfied. Consequently, S_{H^+} varies very much with N_{eff} at intermediate velocities. For a Ag target, the condition $\omega_p=25.0$ eV seems to bring a curve fit to experimental data.[20,24,25,29,30,32–37] Here, we find the following problem: There is a discrepancy between a recommended N_{eff} and the inherent valency of silver ($N_{\text{eff}}=1$). One practical explanation to reconcile these two is that in the outer region of the WS cell, there exist extra electrons, e.g., bonding electrons or a part of core electrons except a free electron, which cause the pile of the electron density in the outer region. Since this is a qualitative discussion, a quantitative one is necessary to get a more detailed understanding. Anyway, if we use the observed ω_p data to determine N_{eff}, the application of the solid LEDM to nonsimple metals often provides good agreement.

So far, we have two types of the LEDM. Figure 6 is drawn to show how many differences there are in the mean excitation energy I by using two LEDM's. Here I is expressed as

$$Z_2 \ln I = \int_0^\infty dr\, 4\pi r^2 \rho(r) \ln[\gamma \omega_p(r)] , \tag{3.1}$$

where γ is a constant which takes into account the pair excitation as well as the collective excitation. Both Lindhard and Scharff[38] and Chu and Powers[39] have used $\gamma=2^{1/2}$, while Wilson *et al.*[40] adopted $\gamma=1.2$ since this approximation reproduces the atomic mean excitation energy calculated by Dehmer *et al.*[41] in the framework of the oscillator strength formalism. Our calculation is performed for $\gamma=2^{1/2}$ since the purpose is only to estimate the difference in I. According to Fig. 6, the solid LEDM yields, on the whole, greater values than the atomic one, and the difference is marked especially for light elements. This increase in the low-Z_2 region is consistent with the other's calculation.[40] Note that crosses and open circles in the figure denote the results for N_{eff}'s obtained from the observed ω_p data[42] and for $N_{\text{eff}}=2$, respectively.

Returning to Eq. (2.1), the CSD inside matter is indispensable in obtaining the stopping powers S for ion beams. Conversely speaking, the master curves of the stopping S reflect the CSD inside solids although the post-foil effect and the surface effect should be discussed. In this paper the case is considered where incident particles pass through solids at relatively high velocities so that the interaction time with the surface is very short. Thus the surface effect can be neglected here. It is widely accepted that the post-foil process is important in the CSD for heavy ions.[2,43] Actually, once the Auger deexcitation process occurs, the net charge of the emerging particle increases by $+1$ because one electron is ejected from it. When such a process takes place, at least, both one inner-shell vacancy and two excited electrons must exist in the emerging ion. In the case of light ion beams such as H or He, this condition is hardly satisfied except at low velocities. We attempt to predict the CSD from the master stopping curve around the energy where the stopping power is maximum. Therefore, the post-foil effect can also be neglected.

Figure 7 shows the stopping cross sections of Al for He^+, He^{2+} and helium-ion beams. Using two sets of the empirical master stopping $S_{\text{He}}^{\text{em}}$ (Ref. 1) and the theoretical stoppings S_{He^+} and $S_{\text{He}^{2+}}$ ($=4S_{\text{H}^+}$) at two different energies, we propose the charge fraction ratio $\phi_{\text{He}^+}/\phi_{\text{He}^{2+}}$ in

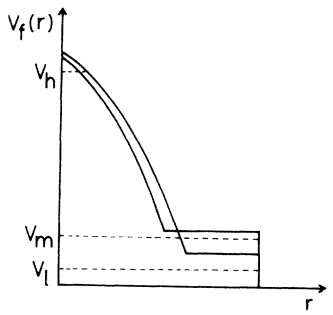

FIG. 5. Schematic representation of the local Fermi velocity $v_F(r)$ for two cases. The velocities v_l, v_m, and v_h denote examples of the low, the middle, and the high velocities of the ion, respectively.

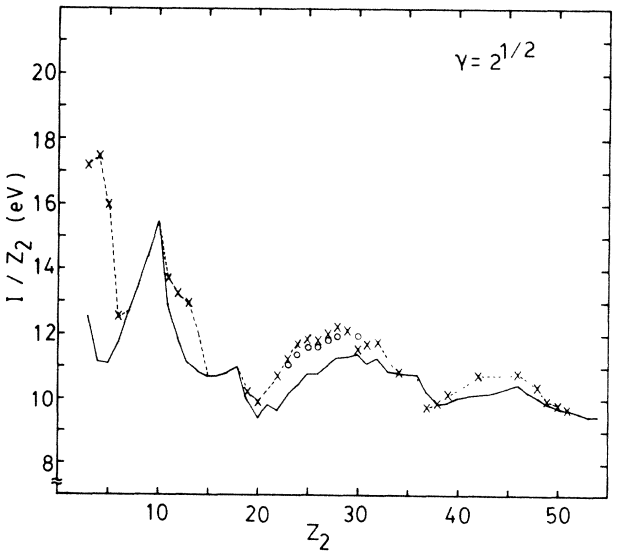

FIG. 6. Calculated mean excitation energy I vs Z_2 number: the atomic LEDM (——), the solid LEDM using the observed ω_p (Ref. 24) (--×--), and the solid LEDM using $N_{\text{eff}}=2$ (○).

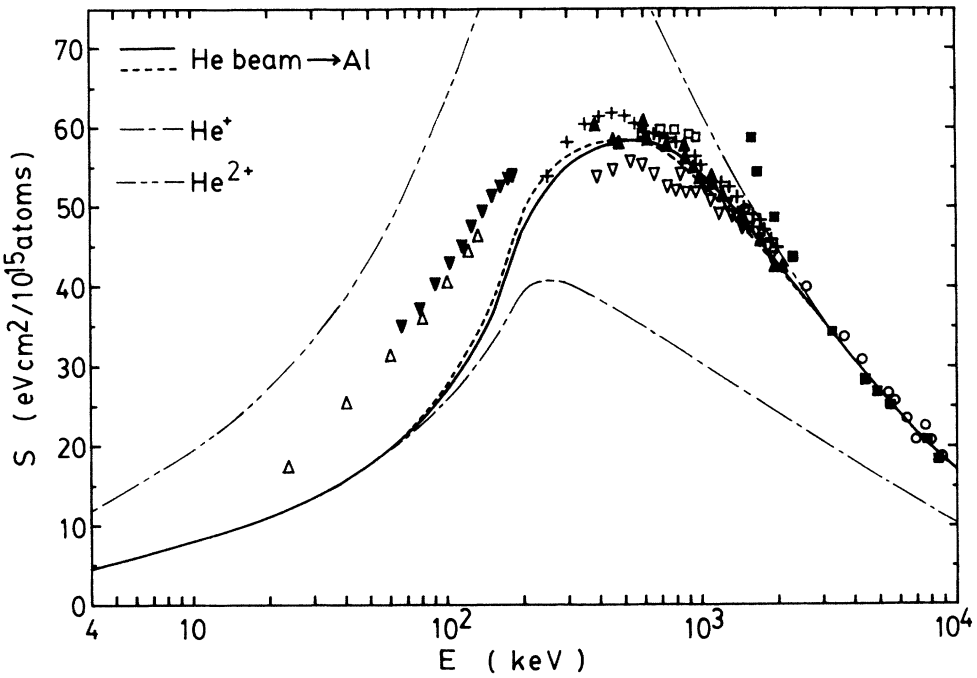

FIG. 7. Stopping cross sections of Al for He: the present results (—— for He-ion beam using the proposed CSD, - - - for He-ion beam using the observed CSD (Ref. 44), —·— for a He^+ ion, and —··— for a He^{2+} ion) and the experimental results (△, Ref. 26; □, Ref. 45; ▽, Ref. 46; ▼, Ref. 47; ■, Ref. 48; ○, Ref. 49; ▲, Ref. 50; +, Ref. 51).

the form (2.5), where $A=0.31$ and $B=1.88$ are obtained and E is measured in units of MeV. Experimentally, the charge fraction ratio was obtained as $\phi_{He^+}/\phi_{He^{2+}} = 0.38E^{-1.60}$ in the energy range $0.6 \leqq E \leqq 2.0$ MeV.[44] A neutral particle He^0 can be ignored due to the screening. The average charge obtained from the present CSD differs from the observed average charge, at most, by 0.04 in the measured energy range. This procedure to propose the

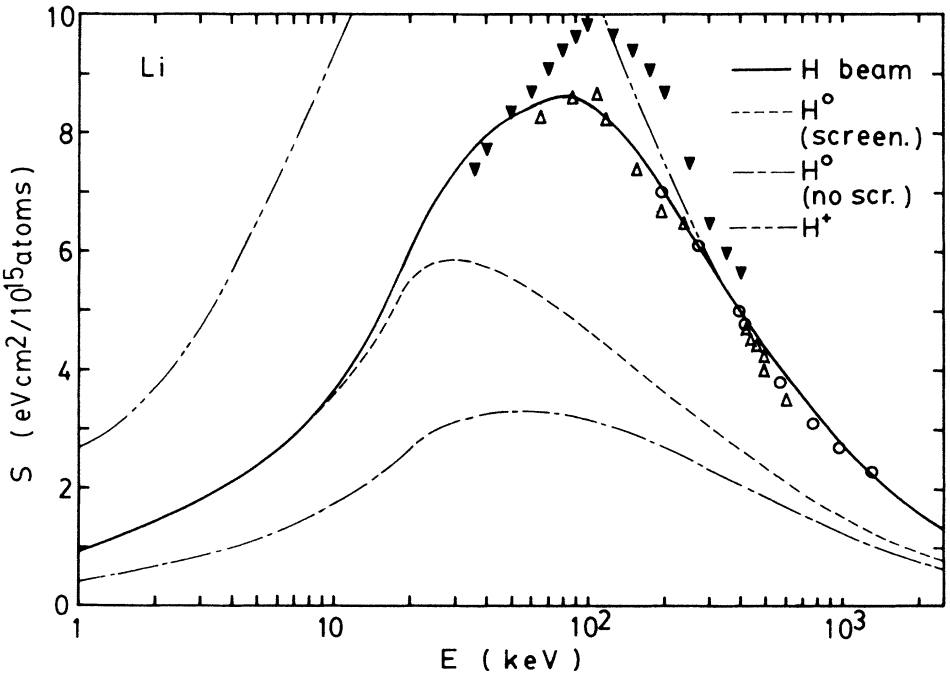

FIG. 8. Stopping cross sections of Li for H: the present results (—— for H beam using the proposed CSD, —·— for a H^+ ion, —··— for a H^0 without the screening effect, and --- for a H^0 including the screening) and the experimental results (△, Ref. 52; ○, Ref. 53; △, Ref. 54).

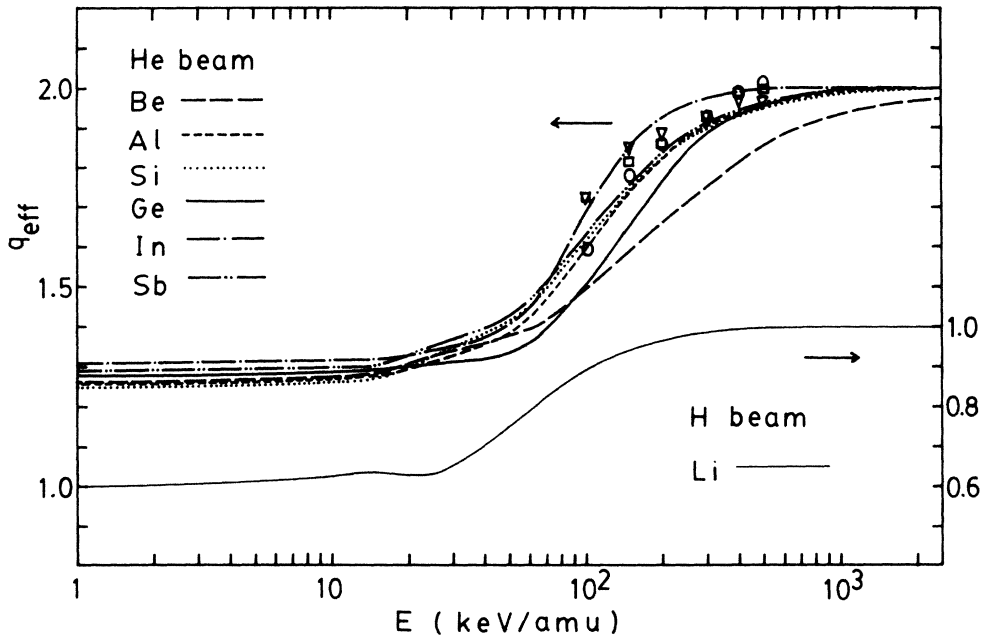

FIG. 9. Calculated effective charge of He beam in Be, Al, Si, Ge, In, and Sb and that of H beam in Li, together with the experimental results (○ in C, □ in Al, and ▽ in Si) (Ref. 29). The arrows indicate the scales of the vertical axes.

CSD is partly supported by the following fact: In the low-energy and the high-energy regions, the calculated S_{He^+} and $S_{He^{2+}}$ values are in good agreement with the data,[26,45–51] respectively. This implies that almost all helium ions with low energies in solids are singly ionized, and all helium ions are fully stripped in the energy region $E \gtrsim 2$ MeV. The screening effect on a He^+ does not change the proposed CSD appreciably. The charge fractions ϕ_{He^+} and $\phi_{He^{2+}}$ fill the role of predicting the stoppings reasonably between ~ 100 keV and a few MeV.

In alkali metals a proton can bind an electron because of their high r_s values. As an example, the stopping cross section of Li is shown in Fig. 8. In a similar way to the He case, the charge fraction ratio for the H case is determined as $\phi_{H^0}/\phi_{H^+} = 5.87 \times 10^{-3} E^{-2.0}$, where E is measured in MeV. The screening effect on a H^0 is significant and resultantly enhances the stopping cross section S_{H^0} by a factor of 2 up to $v \sim v_0$. The extended radius of the bound state in a H^0 in Li is given as $a_1 = 1.579 a_0$, and for other alkali metals, calculated values are presented in Table II. Although there are not enough data,[52–54] the calculated result in the low energies connects smoothly with that in the high energies and is, therefore, expected to give a successful result. Referring to neutral fraction data of a proton,[55] the fraction ϕ_{H^0} of a hydrogen emerging from Li is greater than that from such metals as C, Al, Cr, Ni, and Au, while the energy dependence of ϕ_{H^0} from Li is nearly equal. The feature of the stopping of Li is expected to be valid for other alkali metals.

The formula (2.1) clarifies the problem of how the mean charge of helium-ion beams obtained from the CSD in matter is connected with the effective charge in the stopping. In Fig. 9 the calculated effective charge for He-ion beams, q_{eff}^{He}, in Be, Al, Si, Ge, In, and Sb and that for a proton beam, q_{eff}^{H}, in Li are shown, where q_{eff}^{He} and q_{eff}^{H} are defined as

$$q_{eff}^{He} = (\phi_{He^+} S_{He^+}/S_{H^+} + 4\phi_{He^{2+}})^{1/2} \tag{3.2}$$

and

$$q_{eff}^{H} = (\phi_{H^0} S_{H^0}/S_{H^+} + \phi_{H^+})^{1/2} . \tag{3.3}$$

at energies considered. For low-energy He-ion beams, q_{eff}^{He} directly reflects the square root of the stopping ratio, i.e., S_{He^+}/S_{H^+}, since $\phi_{He^+} \cong 1$. The overall feature of q_{eff}^{He} with respect to energy is consistent with the data[1] except that experiments give a bit larger q_{eff}^{He} values. The inequality $S_{He^+} > S_{H^+}$, being valid over all energy ranges, comes from the size effect of a He^+ ion. This causes a weak Z_2 dependence of q_{eff}^{He}.[10] As regards q_{eff}^{H}, it is less than unity in the low-energy region since hydrogen atoms can exist in Li metal. There, due to the screening effect, q_{eff}^{H} is increased by 40% in comparison with a no-screening case. These remarks will be valid, in general, for alkali metals.

IV. CONCLUSION

The stopping cross sections and the related quantity of solids for protons and helium ions are investigated comprehensively, where the dielectric-function method and the local-electron-density models are used. As well as for point charges H^+ and He^{2+}, the stopping cross sections for a partially stripped ion He^+ are obtained over a wide energy range. The stopping ratio S_{He^+}/S_{H^+} shows a remarkable behavior with respect to specific energy, as shown in Fig. 2. In spite of treating in a simple form, the

screening effect on the stopping for a H^0 is much more significant than for a He^+. The main point of the paper is to include the CSD in matter and to treat particles with the bound electron. Such a procedure as based on Eq. (2.1) already appeared in Ref. 56, where the upper and the lower bounds of the effective helium-ion charge are taken into account instead of the CSD and the size effect of a He^+. When we consider q_{eff} in the stopping, the ion size plays an important role as well as the CSD, resulting in the relation $q_{\text{eff}} > \bar{q}$ ($\bar{q}$ is the average charge) for He-ion beams.[10] Using the theoretical stoppings for H^0, H^+ (and He^{2+}), and He^+ particles, the equilibrium CSD of H and He beams is proposed. In comparing the present CSD with the measured CSD, the post-foil effect and the surface effect are neglected. This neglect is valid for light ion beams with high velocities. As for heavier ions, the above effects will have to be considered. Except for a nonequilibrium charge state, energy losses accompanied by the charge-exchange process, and excited states of ions, the formula (2.1) is also regarded as the starting equation in analyzing the stopping for heavy ion beams. At this stage, Eq. (2.1) is an extension of the procedure used in Ref. 9, where the spatial distribution of the bound electrons of the projectile is determined in a statistical model with the velocity criterion.

ACKNOWLEDGMENTS

The author would like to thank Professor Y. Yamamura and Professor Y. H. Ohtsuki for useful discussions. This work was financially supported by the Special Project Research on Ion Beam Interactions with Solids from Ministry of Education, Science, and Culture, Japan.

[1]J. F. Ziegler, in *The Stopping and Ranges of Ions in Matter*, edited by J. F Ziegler (Pergamon, New York, 1977), Vols. 3 and 4.
[2]H.-D. Betz, Rev. Mod. Phys. **44**, 465 (1972).
[3]H. A. Bethe, Ann. Phys. (Leipzig) **5**, 325 (1930).
[4]F. Bloch, Ann. Phys. (Leipzig) **16**, 285 (1933).
[5]O. B. Firsov, Zh. Eksp. Teor. Fiz. **36**, 1517 (1959) [Sov. Phys.—JETP **9**, 1076 (1959)].
[6]J. Lindhard and A. Winther, K. Dan. Vidensk. Selsk. Mat.-Fys. Medd. **34**, No. 4 (1964).
[7]T. L. Ferrell and R. H. Ritchie, Phys. Rev. B **16**, 115 (1977).
[8]Y. K. Kim and K. Cheng, Phys. Rev. A **22**, 61 (1980).
[9]B. S. Yarlagadda, J. E. Robinson, and W. Brandt, Phys. Rev. B **17**, 3437 (1978); W. Brandt and M. Kitagawa, *ibid.* **25**, 5631 (1982).
[10]T. Kaneko, Phys. Rev. A **30**, 1714 (1984).
[11]E. Clementi and C. Roetti, At. Data Nucl. Data Tables **14**, 177 (1974).
[12]I. Gertner, M. Meron, and B. Rosner, Phys. Rev. A **18**, 2022 (1978); **21**, 1191 (1980).
[13]W. Brandt, in *Atomic Collisions in Solids*, edited by S. Datz, B. R. Appleton, and C. D. Moak (Plenum, New York, 1975), Vol. 1, p. 261.
[14]F. J. Rogers, H. C. Graboske, Jr., and D. J. Harwood, Phys. Rev. A **1**, 1577 (1970).
[15]F. Guinea, F. Flores, and P. M. Echenique, Phys. Rev. B **25**, 6109 (1982).
[16]M. C. Cross, Phys. Rev. B **15**, 602 (1977).
[17]T. Kaneko, Nucl. Instrum. Methods B **2**, 491 (1984).
[18]Such a treatment was first discussed by K. B. Winterbon [Nucl. Instrum. Methods **144**, 311 (1977)].
[19]Within the framework of nonlinear screening, it is possible for a H^- ion to exist inside solids with $r_s > 1.9$ [see the following reference: C. O. Almbladh, U. von Barth, Z. D. Popovic, and M. J. Scott, Phys. Rev. B **14**, 2250 (1976)].
[20]A. Johansen, S. Steenstrup, and T. Wohlenberg, Radiat. Eff. **8**, 31 (1971).
[21]J. H. Ormrod, J. R. Macdonald, and H. E. Duckworth, Can. J. Phys. **43**, 275 (1965).
[22]S. D. Warshaw, Phys. Rev. **76**, 1759 (1949).
[23]R. L. Wolke, W. N. Bishop, E. Eichler, N. R. Johnson, and G. D. O'Kelley, Phys. Rev. **129**, 2591 (1963).
[24]H. H. Andersen, C. C. Hanke, H. Sørensen, and P. Vajda, Phys. Rev. **153**, 338 (1967).
[25]K. Morita, H. Akimune, and T. Suita, J. Phys. Soc. Jpn. **22**, 1503 (1967).
[26]W. White and R. M. Mueller, J. Appl. Phys. **38**, 3660 (1967).
[27]D. Kahn, Phys. Rev. **90**, 503 (1953).
[28]E. P. Arkhipov and Yu. V. Gott, Zh. Eksp. Teor. Fiz. **56**, 1146 (1969) [Sov. Phys.—JETP **29**, 615 (1969)].
[29]D. C. Santry and R. D. Werner, Nucl. Instrum. Methods **188**, 211 (1981).
[30]E. I. Sirotinin, A. F. Tulinov, V. A. Khodyrev, and V. N. Mizguin, Nucl. Instrum. Methods B **4**, 337 (1984).
[31]M. Inokuti, J. L. Dehmer, T. Baer, and J. D. Hanson, Phys. Rev. A **23**, 95 (1981).
[32]A. Valenzuela, W. Meckbach, A. J. Kestelman, and J. C. Eckardt, Phys. Rev. B **6**, 95 (1972).
[33]D. W. Green, J. N. Cooper, and J. C. Harris, Phys. Rev. **98**, 466 (1955).
[34]J. C. Eckardt, Phys. Rev. A **18**, 426 (1978).
[35]E. I. Sirotinin, A. F. Tulinov, A. Fiderkevich, and K. S. Shyshkin, Radiat. Eff. **15**, 149 (1972).
[36]A. Nomura and S. Kiyono, J. Phys. D **8**, 1551 (1975).
[37]P. Bauer, D. Semrad,and R. Golser, Nucl. Instrum. Methods B **2**, 149 (1984).
[38]J. Lindhard and M. Scharff, K. Dan. Vidensk. Selsk. Mat.-Fys. Medd. **27**, No. 15 (1953).
[39]W. K. Chu and D. Powers, Phys. Lett. **40A**, 23 (1972).
[40]J. W. Wilson, C. K. Chang, Y. J. Xu, and E. Kamaratos, J. Appl. Phys. **53**, 828 (1982); J. W. Wilson and Y. J. Xu, Phys. Lett. **90A**, 253 (1982); J. W. Wilson and E. Kamaratos, *ibid.* **85A**, 27 (1981).
[41]J. L. Dehmer, M. Inokuti, and R. P. Saxon, Phys. Rev. A **12**, 102 (1975).
[42]D. Pines, Rev. Mod. Phys. **28**, 184 (1956).
[43]W. N. Lennard, D. Phillips, and D. A. S. Walker, Nucl. Instrum. Methods **179**, 413 (1981).
[44]Y. Haruyama, Y. Kanamori, T. Kido, and F. Fukuzawa, J. Phys. B **15**, 779 (1982); Y. Haruyama, Y. Kanamori, T. Kido, A. Itoh, and F. Fukuzawa, *ibid.* **16**, 1225 (1983).
[45]D. I. Porat and K. Ramavataram, Proc. R. Soc. London, Ser. A **252**, 394 (1959).
[46]W. K. Chu and D. Powers, Phys. Rev. **187**, 478 (1969).
[47]R. D. Moorhead, J. Appl. Phys. **36**, 391 (1965).
[48]H. Nakata, Can. J. Phys. **47**, 2545 (1969).
[49]J. R. Comfort, J. F. Decker, E. T. Lynk, M. O. Scully, and A. R. Quinton, Phys. Rev. **150**, 249 (1966).

[50]J. S.-Y. Feng, J. Appl. Phys. **46**, 444 (1975).
[51]D. C. Santry and R. D. Werner, Nucl. Instrum. Methods **178**, 523 (1980).
[52]M. Bader, R. E. Pixley, F. S. Mozer, and W. Whaling, Phys. Rev. **103**, 32 (1956).
[53]W. D. Warters, W. A. Fowler, and C. C. Lauritsen, Phys. Rev. **91**, 917 (1953).
[54]L. J. Haworth and L. D. P. King, Phys. Rev. **54**, 48 (1938).
[55]A. Chateau-Thierry and A. Gladieux, in *Atomic Collisions in Solids,* edited by S. Datz, B. R. Appleton, and C. D. Moak (Plenum, New York, 1975), Vol. 1, p. 307.
[56]B. M. Latta and P. J. Scanlon, Phys. Rev. A **12**, 34 (1975).